

DAA/LANGLEY  
NAG1-424

10-34

63683

27P.

VISCOS FLOW DRAG REDUCTION

BY ACOUSTIC EXCITATION

Final Report

Dr. Robert T. Nagel  
Principal Investigator  
Mechanical and Aerospace Engineering  
Campus Box 7910  
North Carolina State University  
Raleigh, North Carolina 27695-7910

Grant Number NAG-1-424 ✓

NASA Technical Officer: John B. Anders

(NASA-CR-180298) VISCOS FLOW DRAG  
REDUCTION BY ACOUSTIC EXCITATION Final  
Report (North Carolina Univ.) 27 p Avail:  
NTIS BC A03/MF A01 CSCL 20D

N87-27123

Unclassified  
G3/34 0063683

### Introduction

The outer part of a turbulent boundary layer is dominated by large eddies<sup>1</sup> with typical length scales of the order of the boundary layer thickness  $\delta$ . The large scale structure is convected downstream with a velocity,  $U_C$ , approximately equal to 0.93 times<sup>2</sup> the free stream velocity  $U_0$ . Passing of the large eddies is semiperiodic<sup>3</sup> with an expected period of approximately  $2.5 \delta/U_0$ . Large eddies are associated with the transfer of momentum to the wall and are related to the skin friction production phenomena although the mechanism for the linkage is unclear<sup>4,5,6</sup>.

Early boundary layer manipulation<sup>7</sup> was first performed by positioning mesh screens inside the layer. This caused the destruction of the large eddies and a skin friction drag reduction downstream of the screens. The drag of the device itself was, however, excessive. This initial work lead to a series of investigations by Hefner et al.<sup>8</sup>, Corke et al.<sup>9,10</sup>, Bertelrud et al.<sup>11</sup> and others. The result of these many efforts has produced an evolution in large eddy break up devices (LEBU's) which suggests tandem blades as an effective configuration.

In recent investigations<sup>12,13</sup>, net drag reduction was achieved with optimized plate manipulators and airfoil shaped large eddy break-up devices. It should be mentioned that repeatability of net drag reduction due to large eddy destruction is generally unsatisfactory<sup>14</sup> and that the micro-geometry of the plate manipulators is critical<sup>15</sup>.

The focus of this study is to enhance the effectiveness of a single blade manipulator configuration. It is assumed that large eddies impinging upon a LEBU plate generate unsteady lift forces due to the variation of the effective angle of attack. The mechanism of large eddy cancellation by the LEBU blade is assumed to be a vortex cancellation process<sup>16,17</sup>. Because of the unsteady

circulation around the device, vortices are shed from its trailing edge. The oncoming large eddies in the boundary layer interact with the shed vorticity and are assumed to be partially canceled.

This paper describes an experimental program in which the effectiveness of a single LEBU blade is enhanced by proper acoustic excitation. The acoustic waves are generated in response to the incident large scale eddies and directed at the blade trailing edge through the test surface floor below the manipulator blade. The acoustic input is phase locked to the incident flow. Control of the acoustic input apparently allows enhancement of the large eddy cancellation process leading to a decrease in skin friction coefficient  $C_f$ . Control of this process with acoustic excitation indicates that vortex unwinding is the mechanism for large eddy destruction in the boundary layer. A deeper understanding of the phenomena could lead to better drag reduction technology and further understanding of the physics of the turbulent boundary layer.

#### Basic Experimental Apparatus

The experimental study was conducted in the recently constructed NCSU Boundary Layer Wind Tunnel<sup>18</sup>. This facility features: a long test section (~7.0 m) to achieve high Reynolds Numbers at low speeds, a velocity range from 4.0 to 33.0 m/s and extremely uniform mean flow with turbulence intensities less than 0.25 percent. A single LEBU blade was carefully fabricated from stainless steel shimstock and mounted at a distance of 2.0 m from the leading edge of the test section (figure 1). The manipulator extends through the walls of the test section at a height above the wind tunnel floor equal to 90 percent of the local boundary layer thickness. The device was mounted outside of the test section with accurate control over the LEBU's height, angle of attack and tension. Independent adjustment of both ends of the device is possible. The mount stands independently from the wind tunnel to eliminate possible

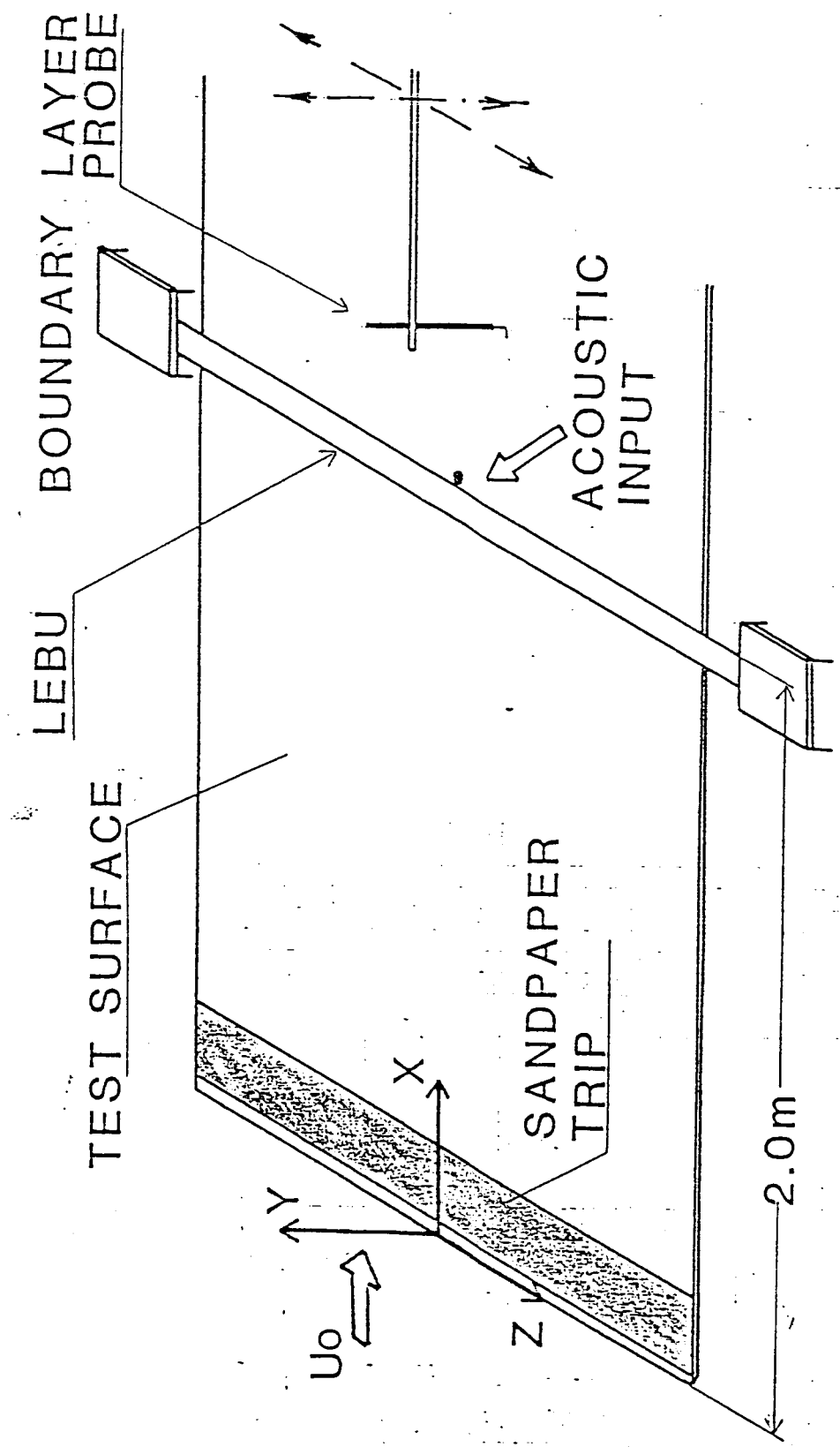


Fig. 1. Large Eddy Break Up Device and flat test surface.

vibrations of the stretched plate. The LEBU extends through openings in the wind tunnel side walls across the full span of the test section. A sandpaper type trip is mounted starting 4.0 cm from the leading edge of the test section floor and extending 21.0 cm downstream. The trip quickly establishes a fully developed turbulent boundary layer with a complete range of length scales. Details of the flow are available in reference 18.

Measurements of the boundary layer profile downstream of the manipulator plate were obtained using a small boundary layer pitot probe (0.5 mm outside diameter). A remotely controlled traversing mechanism was used to assist with accurate probe positioning. The traversing device provides probe movement over the Y-Z plane in the wind tunnel test section (figure 1) with a positioning accuracy of  $\pm 0.1$  mm. The pressures from the boundary layer probe were measured with a differential pressure transducer while static pressure was obtained from taps in the test surface. Approximately 200 samples were obtained and averaged at each point and the velocity profile was determined by 40 such points. A Digital 16 bit resolution data acquisition system was utilized to process the measured data and monitor the tunnel operation.

The momentum thickness,  $\theta$ , is calculated from its definition by numerically integrating the appropriate function of the velocity profile over the boundary layer thickness. For zero pressure gradient two-dimensional flow Von Karman's Momentum Integral Equation reduces to:

$$C_f/2 = d\theta/dx , \quad (1)$$

where  $C_f$  is the local skin friction coefficient and  $x$  is the axial direction. The momentum thickness,  $\theta$ , is determined as described above for a plurality of positions downstream of the LEBU. The values can be fit to a power curve of the form:

$$\theta = ax^b \quad (2)$$

Hence, the skin friction coefficient is represented by

$$C_f = 2.0 abx^{(b-1)}. \quad (3)$$

This expression provides only an average magnitude and x-dependence.

The momentum thickness,  $\theta$ , is of primary interest because it represents both  $C_f$  and the net drag in the entire shear layer region, including the drag of the manipulator plate. Figure 2 shows measured and theoretical values of  $\theta$  versus downstream distance  $x$  for the baseline case of the boundary layer without manipulation. The solid line represents a prediction by Head's Method<sup>19</sup>. Head's Method was applied for zero pressure gradient flow and was initialized at the end of the sandpaper trip with a momentum thickness predicted using an empirical formula from White<sup>20</sup> and an assumed shape parameter  $H = 1.375$ . The experimental values were obtained by averaging 3 points across the span of the test surface. Agreement between the predicted and measured values was found satisfactory with a maximum deviation of 3 percent.

The velocity profile for the plain flow configuration was compared to a modified Coles' profile<sup>19</sup> at an axial location 2.5 m from the test section leading edge. The maximum deviation between predicted and measured velocity, figure 3, was 2 percent. The baseline flow without a boundary layer manipulator is thus a classic fully developed turbulent boundary layer on a flat plate.

The experimental arrangement to acoustically excite the LEBU trailing edge is shown in figure 4. A hot film probe is positioned upstream of the LEBU device at the LEBU height. The signal from the sensor is output from an anemometer into a specially designed processor. The processor responds only to large excursions of the hot film signal. The threshold level,  $V_T$ , which triggers a response from the processor is adjustable. This adjustment allows

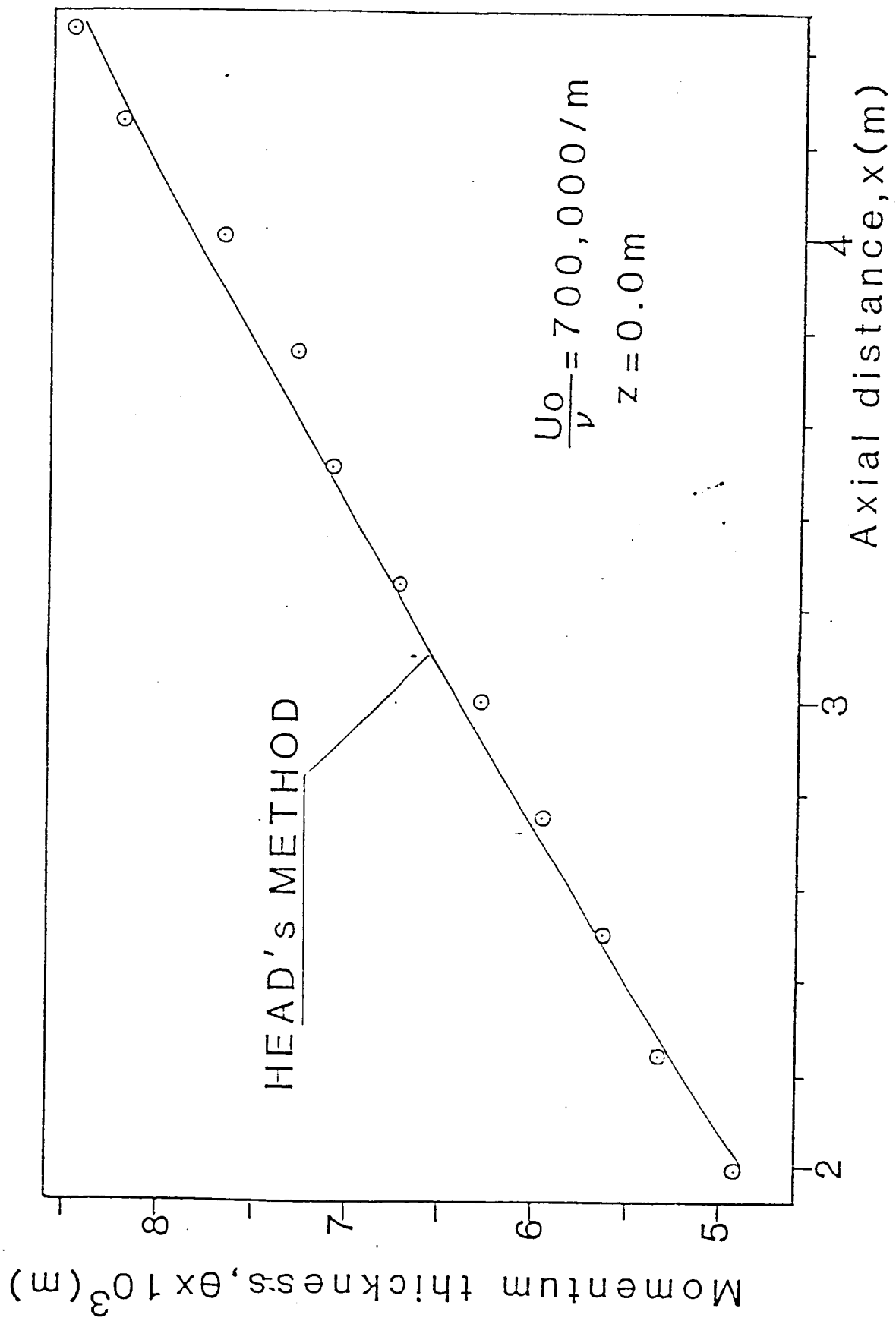


Fig. 2. Growth of predicted and measured momentum thickness,  $\theta$ , for the plain flow case.

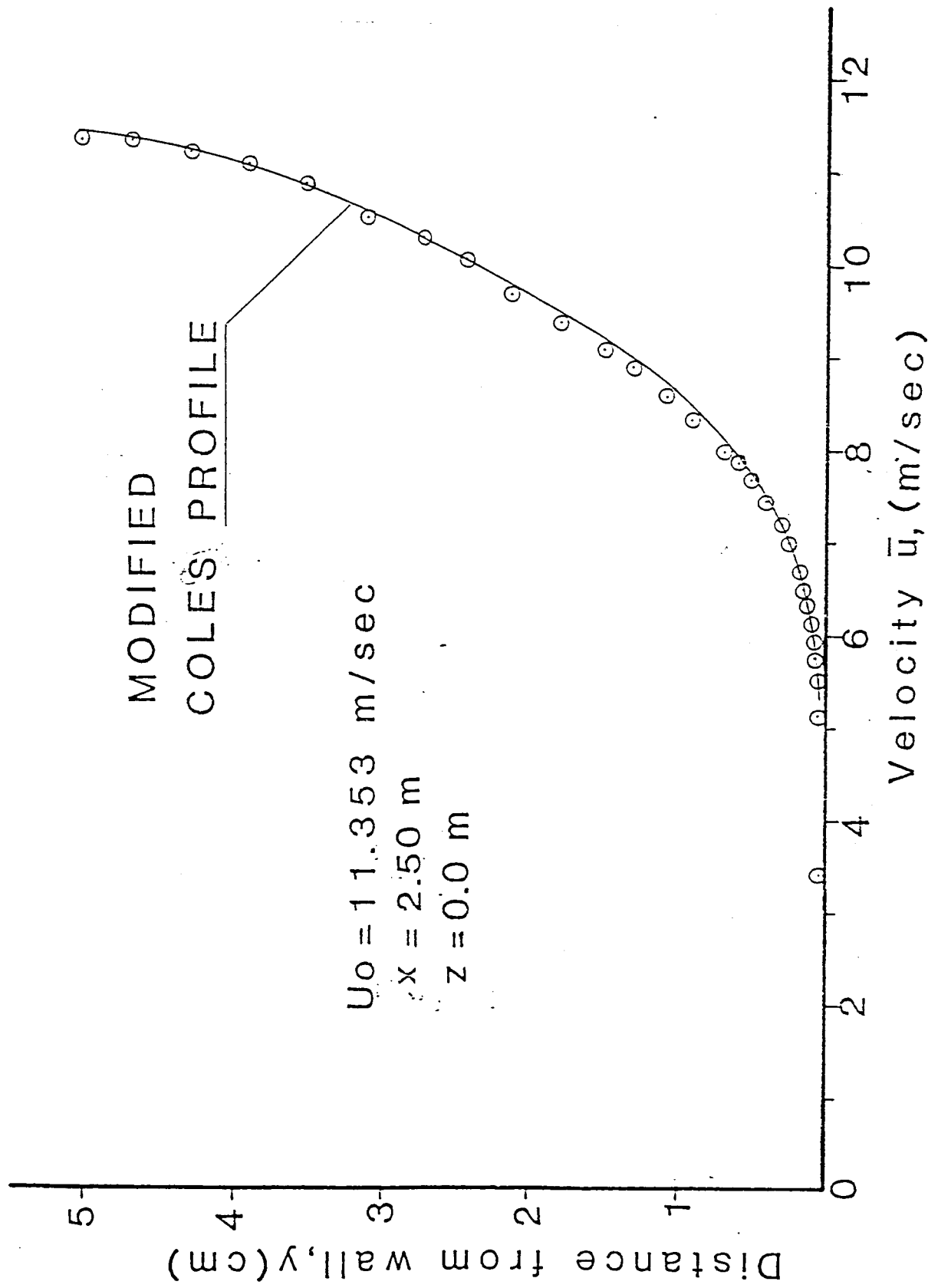


Fig. 3. Predicted velocity  $\bar{u}$ , m/sec and measured mean velocity profile for plain flow configuration.

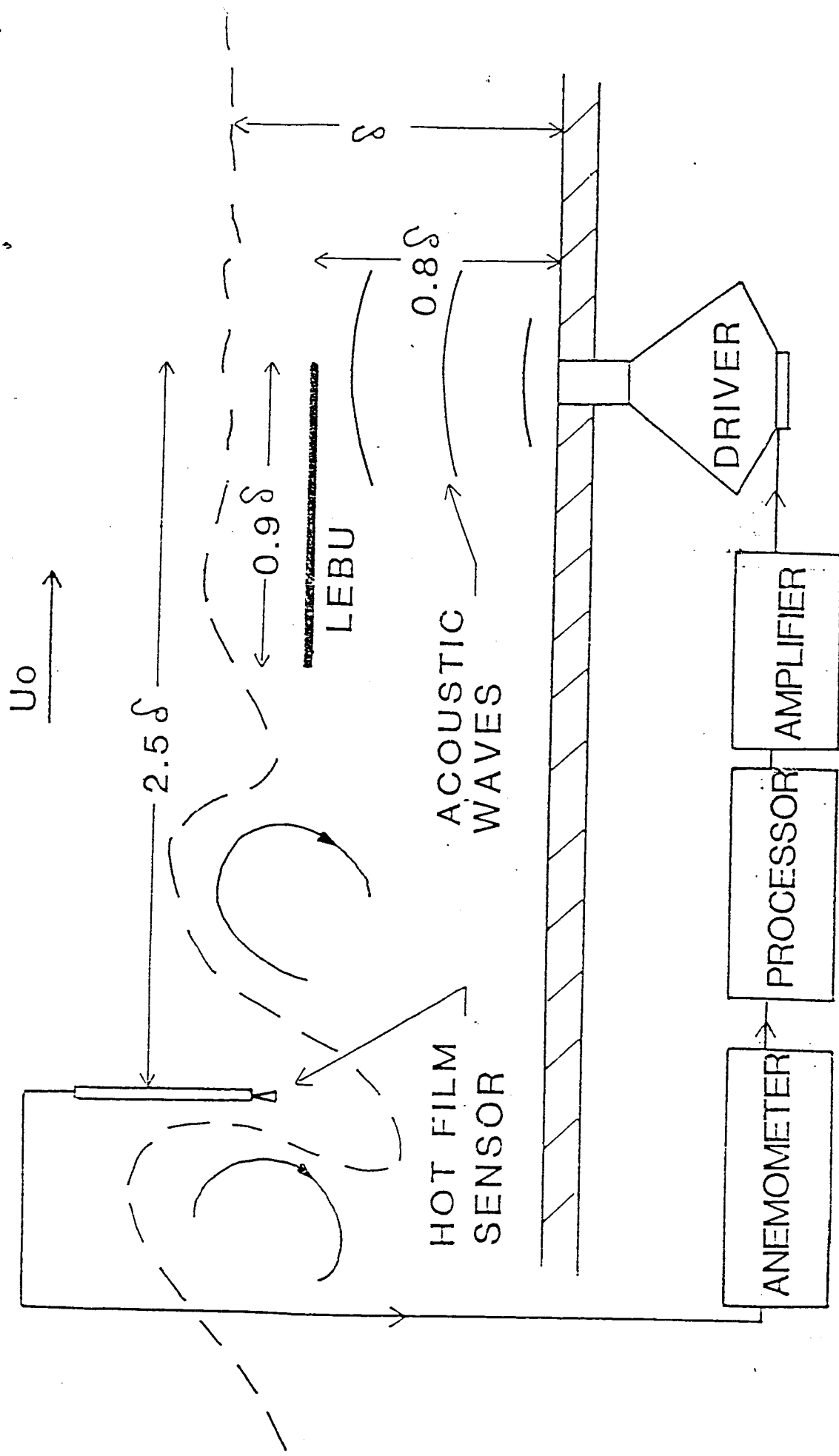


Fig. 4. Schematic representation of the acoustic excitation mechanism.

selection of a lower limit of large scale eddies to which the processor will respond. Eddies with velocity fluctuations below this threshold level are ignored while eddies with associated velocity excursions beyond the threshold level produce a response from the processor. The response is a signal with character and duration equal to the anemometer's large fluctuations as shown on the dual trace oscilloscope display of figure 5. The response of the processor must also be time delayed and amplified. The time delay,  $t$ , is set equal to the large eddy convection time between the upstream hot film sensor and the LEBU trailing edge.

The processor response is then used to drive acoustic waves from a location on the floor of the wind tunnel below the trailing edge of the LEBU. The acoustic waves can therefore be made to arrive at the LEBU trailing edge together with the incident large eddies. In this manner the vorticity shed from the LEBU, which apparently influences the eddy cancellation, can be modified. The pressure pulse device consists of an 8 inch woofer speaker which is seal mounted on the wide side of a conical channel.

#### Operating Conditions

The spatial and temporal variation of the test section mean flow is approximately 0.2 percent while the momentum thickness across the test section span varied less than 4 percent of the mean value. These small deviations combined with the measured flow characteristics allow the assumption of a two dimensional ergodic turbulent boundary layer.

The wind tunnel velocity is set for a unit Reynolds Number of  $700,000/m$ . The corresponding typical mean flow velocity is approximately 11m/s and the Reynolds Number based upon the momentum thickness at the LEBU location is about 3,100. The boundary layer thickness,  $\delta$ , at the LEBU location is

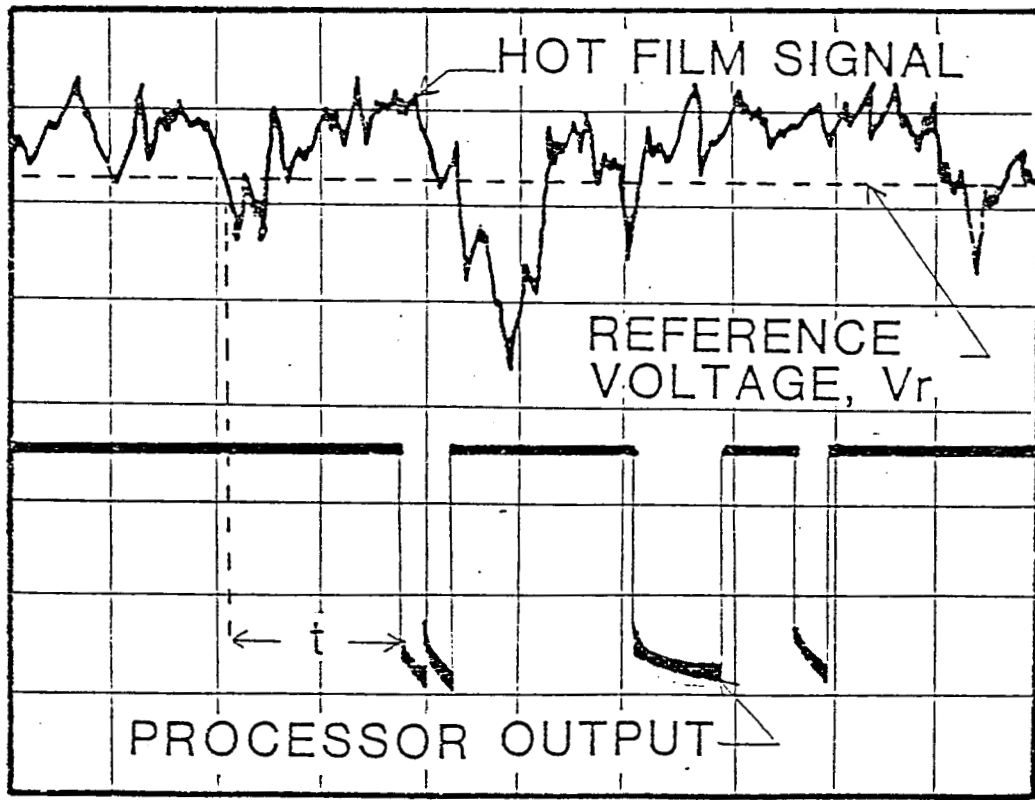


Fig. 5. Time delayed processor response to incident flow,  
[2 volts/div., 5 msec/div.].

approximately 4.0 cm. The LEBU chord length is  $\sim 0.90\delta$ , its height above the test surface is  $\sim 0.8\delta$ , and its thickness is  $\sim 0.005\delta$ . These dimensions comply with the recommendations of reference 14.

The upstream hot film probe was positioned at midspan of the test surface at a height of  $0.85\delta$ , and at a distance,  $s$ , of  $2.45\delta$  upstream of the LEBU trailing edge. This probe, used to detect the incident eddies, was positioned as close as possible to the LEBU trailing edge because the large eddies lose their coherence<sup>2</sup> after a distance of about  $4\delta$ . The location of the large eddy detector probe must be, however, far enough upstream in order to prevent a feedback from the acoustic pulses. At this location the eddy detector probe did not respond to the acoustic input. The axis of the probe support was inclined at 45 degrees with respect to the test section vertical plane of symmetry to avoid probe interference with the downstream flow field. The processor response was set at  $t = s/0.93U_0$ ; a typical value of  $t$  was 10 msec.

The pressure pulse mechanism was mounted under the test surface at midspan below the LEBU device trailing edge. The acoustic input was directed to the LEBU trailing edge through a circular opening (3/8 inch diameter) covered with fine screen flush mounted to the test surface. A first approximation for the required sound pressure level of the acoustic waves was obtained by considering the boundary layer pressure perturbations near the trailing edge of a flat plate. Reference 21 provides a method to predict the perturbation pressure at the trailing edge of a flat plate in an inviscid flow. The theory of asymptotic expansions is used to solve the Navier-Stokes equations for a laminar boundary layer on the plate. The fluctuating pressure at the thin plate trailing edge was predicted to be 99.9 dB for the given conditions. This is not the pressure fluctuation generated by an oncoming eddy, but rather the typical pressure fluctuation at that location. It was decided, therefore, to

input an acoustic pressure pulse with a time mean of 100 dB. The device was adjusted using a sine wave input and the RMS signal from 0 to 2000 Hz was measured at grazing incidence above the acoustic output port at the LEBU's height.

#### Results and Discussion

Turbulent boundary layer velocity profiles were obtained at midspan locations downstream of the LEBU manipulator. The momentum thickness,  $\theta$ , was calculated and plotted versus downstream distance,  $x$ , from the test surface leading edge. Figure 6 shows the axial variation of  $\theta$  for:

- i. plain flow with the upstream eddy detector sensor installed but not operating,
- ii. the LEBU configuration (upstream sensor installed but not operating) and
- iii. the LEBU configuration with acoustic excitation.

The momentum thickness for the plain flow case, without the large eddy break-up device installed, was also measured with acoustic excitation applied. The eddy detector, signal processor and acoustic input are independent from the LEBU. The resulting data are nearly identical to that of the plain flow case without excitation. When acoustic excitation is applied to the plain flow case the average momentum thickness increases, by less than 0.5 percent. This nearly negligible increase can be compared to reductions in momentum thickness that occur when acoustic excitation is applied to the LEBU. The excited plain case data has therefore been omitted from figure 6 for the sake of clarity.

The momentum thickness of the manipulated flow is greater than the plain flow case because of momentum loss imposed by the embedded thin plate. The momentum thickness near the LEBU trailing edge (4 boundary layer thicknesses

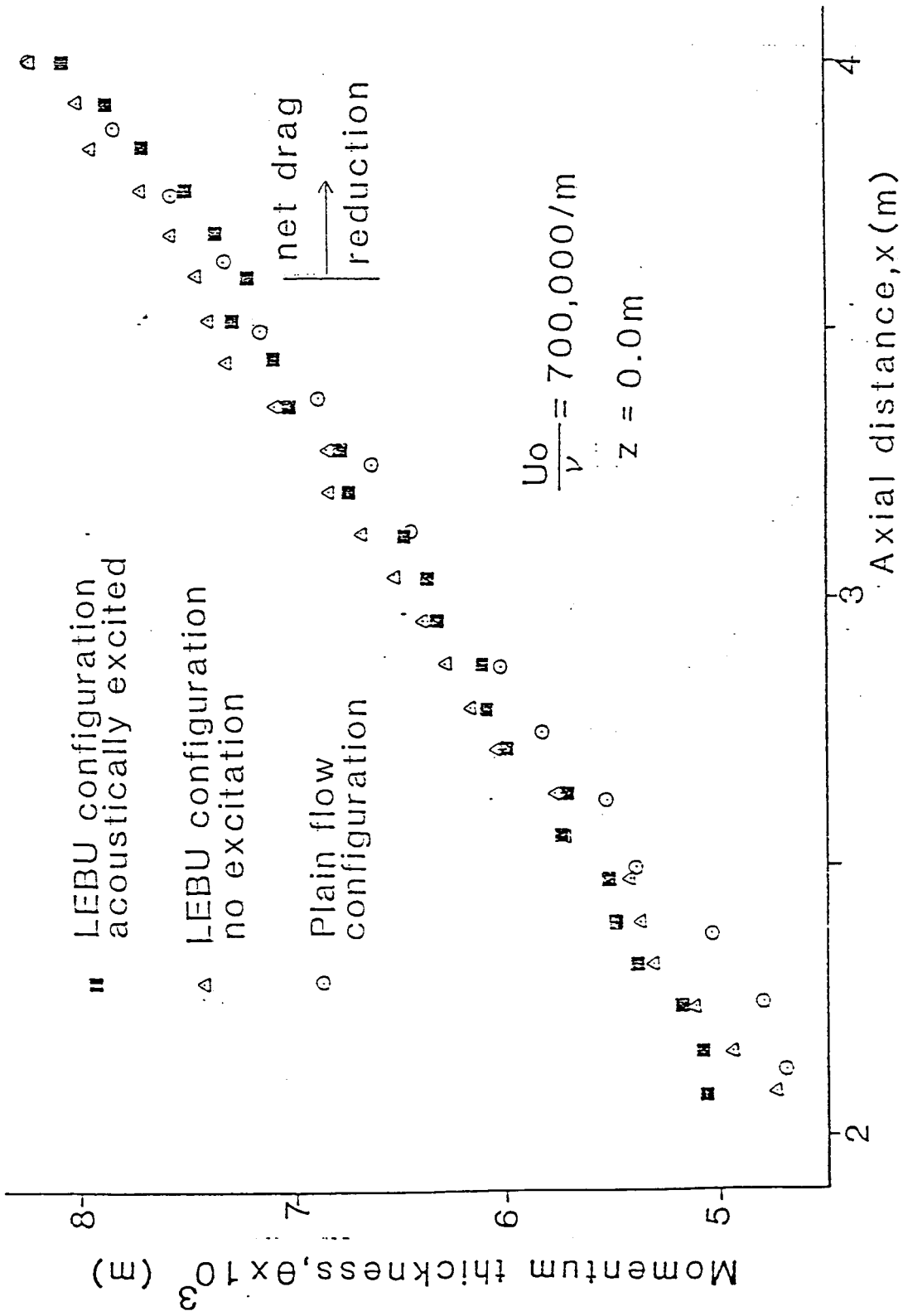


Fig. 6. Momentum thickness,  $\theta$ , versus axial distance  $x$ , for various flow configurations.

downstream) is within 5 percent of the sum of the momentum thickness of the plain flow case and the momentum thicknesses of the laminar boundary layers predicted to develop on the surface of the plate.

The acoustically excited case produces an even greater momentum loss at this location. If the acoustic input was merely tripping the laminar boundary layer, one might hope to repeat the above momentum tabulation using turbulent boundary layers on the LEBU plate. The measured increase in  $\theta$  with the acoustic input is, however, approximately ten times the expected increase that could be attributed to turbulent boundary layers. These results suggest an additional mechanism may be active during the acoustic excitation.

Further downstream at  $x = 2.6$  m (156 from the LEBU) the momentum thickness of the acoustically excited configuration relaxes to that of the unexcited LEBU and grows at a slower rate. The same trend is noted at  $x = 3.8$  m where the momentum thickness of the acoustically excited flow becomes less than the plain flow configuration. This is a clear indication of reduced skin friction coefficient.

The momentum thickness can be used to calculate the total drag coefficient at this point<sup>22</sup>. To do so, a momentum balance is applied using a control volume bounded by the test surface and the undisturbed flow and extending from the test surface leading edge to the axial location  $x$ . The total drag coefficient is then given by:

$$C_D(x) = 2.0\theta(x)/x \quad (4)$$

Figure 6 must then be reconsidered noting that the momentum thickness for an acoustically excited LEBU flow is lower than the other configurations at axial locations beyond about 1.8 m from the LEBU's trailing edge. The net drag reduction is evident.

The variation of skin friction coefficient,  $C_f$ , versus the axial distance from the test surface leading edge is shown in figure 7. All measurements were obtained along the test surface midspan. These points are aligned with the upstream sensor and the acoustic input point. The unexcited LEBU configuration and the acoustically excited LEBU configuration should be compared to the plain flow. The hot film eddy detector sensor was installed for all configurations. All least square curve fits had a correlation coefficient above 0.99. According to the values of the skin friction coefficient, acoustic excitation can enhance the LEBU's effect by reducing  $C_f$  an additional 7 to 15 percent below the unexcited case. Comparison to the plain flow shows a reduction of the wall shear stress between 9 and 19 percent.

Limited data were obtained at various spanwise locations. These data, which will be discussed in a later paper, show that the beneficial effects of acoustic excitation are confined to a narrow region downstream of the acoustic excitation point. The region of increased drag reduction caused by excitation spreads with a half angle of about 2 1/2 degrees.

Space-time cross correlation functions (CCF) were obtained using the hot film eddy detector probe upstream of the LEBU plate as a fixed reference location and another hot film probe at several downstream locations. A dual channel TSI anemometer was utilized and the hot film probe output signals were processed with a Nicolet 660B FFT analyzer.

Figure 8 shows peak values of the space-time cross correlation functions versus probe separation distance,  $d$ , at various distances from the LEBU trailing edge near the outer edge of the boundary layer. When the downstream probe is located upstream of the LEBU, the acoustic input causes small increases in the cross correlation functions because the probes are exposed to

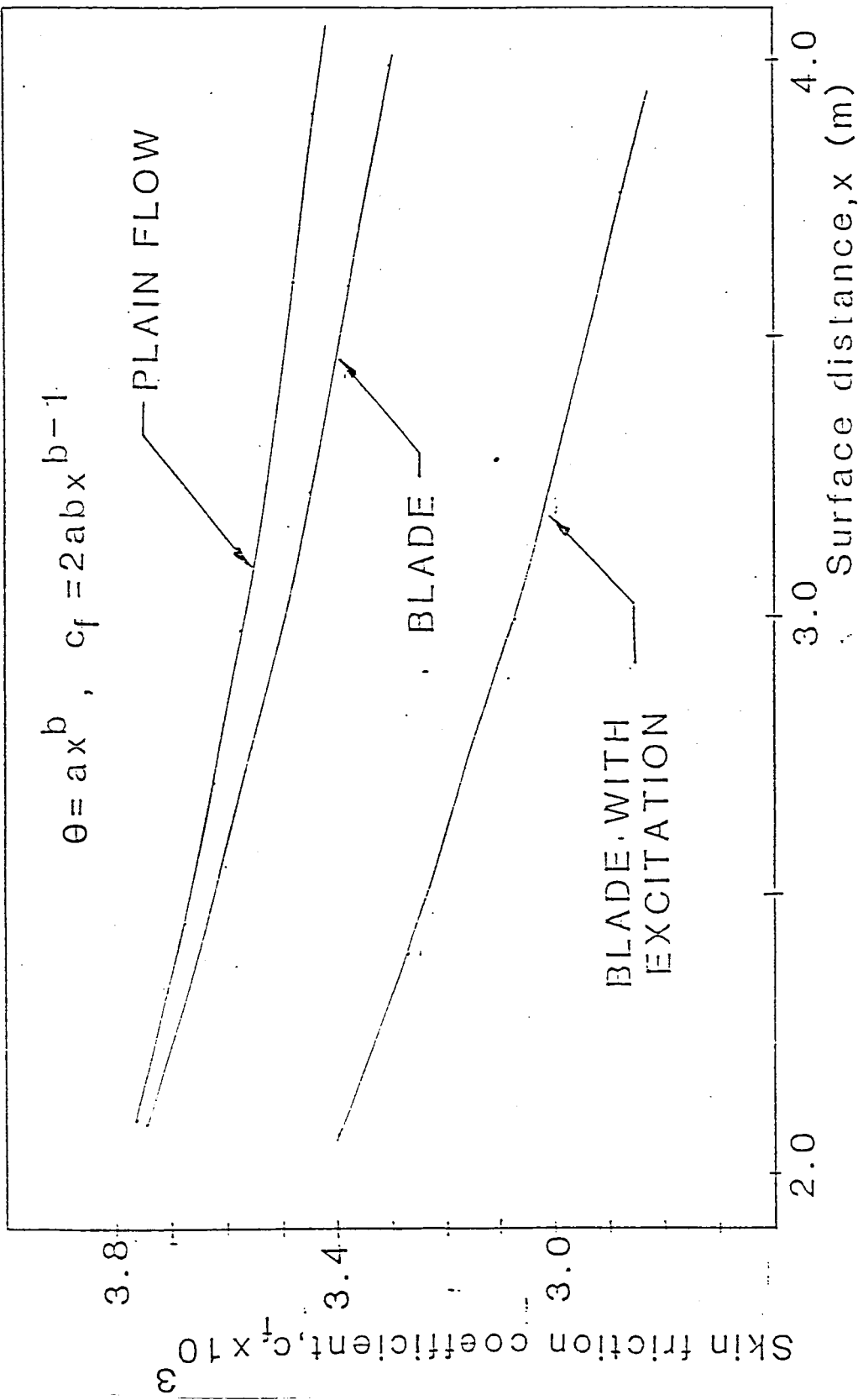


Fig. 7 Variation of the skin friction coefficient,  $C_f$ , for each configuration.

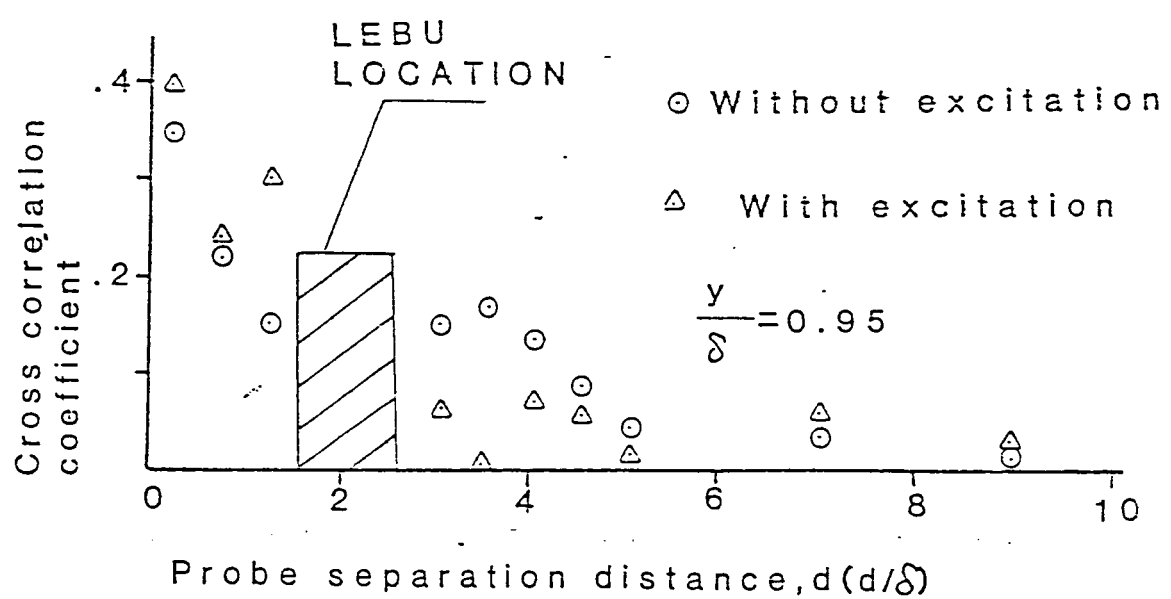


Fig. 8. Maximum space-time velocity cross correlation in the outer part of the boundary layer.

both the large scale eddies and the acoustic field. The correlation peak is associated with the eddy convection time and not the acoustic wave propagation time. At the trailing edge of the plate, the flow without excitation maintains a maximum CCF approximately equal to that observed at the leading edge. The wake of the LEBU in this case is clearly correlated to the incident flow. The time of maximum cross correlation again corresponds to the eddy convection time. When acoustic excitation is applied, the downstream flow is less correlated to the upstream point. This indicates that acoustic excitation of the LEBU enhances the destruction of the large eddies which are sensed at the upstream location. At locations further downstream, the peak CCF are quite small but the acoustically excited case exhibits slightly higher values than the unexcited case.

The values of the CCF are different when the downstream probe is emerged deeper into the boundary layer as shown in figure 9. Just below the height of the LEBU, figure 9a, the addition of acoustic excitation has a very limited effect. The reduction of the CCF is approximately the same as the unexcited case. These data indicate that the phase locked excitation influences the outer region of the boundary layer whereas the unexcited LEBU tends to influence a region slightly closer to the wall. Figure 9b indicates little influence from either the unexcited or excited LEBU at a probe height of approximately 60 percent of the boundary layer thickness. In figure 9b the flow has passed under the manipulator device. The effects of the LEBU and the acoustic excitation upon the LEBU originate near the LEBU trailing edge. It should be noted that the upstream probe was the eddy detector probe and remained in a fixed location for all data of figures 8 and 9. Furthermore, all time delay values associated with the cross correlation function peaks correspond to expected large eddy convection times.

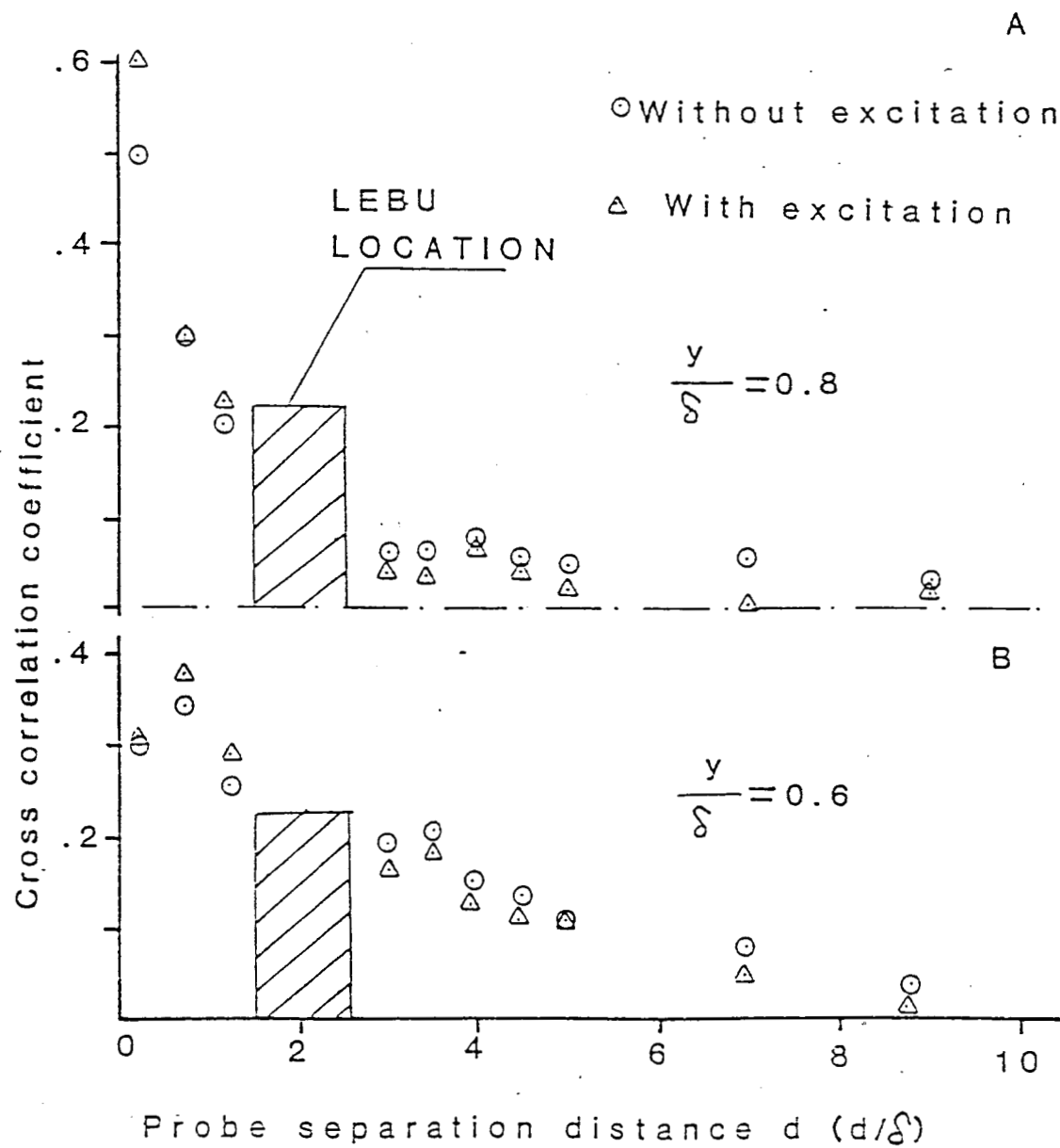


Figure 9. Maximum space-time velocity cross correlation inside the boundary layer.

Turbulence intensity in the low frequency part of the spectrum was examined downstream of the manipulator plate. A hot film probe was positioned slightly above (1.5 mm) the LEBU's height and the turbulence spectrum was measured from 0 to 2000 Hz. Figure 10 compares the RMS value of turbulence for the acoustically excited flow to the unexcited LEBU configuration at several downstream points. The low frequency turbulence is considerably reduced for a distance of  $8\delta$  downstream of the LEBU when acoustics are applied. When the low frequency part of this signal (0 to 200 Hz) is examined, the level of the turbulence intensity appears further reduced. This range of frequencies corresponds to large eddy passing which would occur near 110 Hz and dominate the low frequency spectrum. The relatively higher frequencies (200 to 2,000 Hz) remain largely unaffected by the acoustic input. Only the large wavelengths of the turbulent boundary layer are directly affected when the flow is acoustically excited. The measurements of the RMS velocity fluctuation were limited to a distance of about  $10\delta$  downstream of the LEBU.

Further downstream, within the area of excitation influence, subtle changes in the boundary layer are observed. For example, in the region of net drag reduction the RMS fluctuation of the streamwise velocity component is slightly reduced over the entire thickness of the boundary layer. This is indicative of changes in the shear stress distribution.

To better understand the influence of the flow manipulation, a pulsed smoke wire was used to obtain flow visualization photographs. The smoke wire was mounted downstream of the manipulator at midspan in the tunnel. The fine wires ran vertically from the wind tunnel floor through the boundary layer. Figure 11 shows typical results for the three cases of concern. The large eddy break-up device reduces the large scale structure in the boundary layer and acoustic excitation of the device causes further reduction in coherent motion.

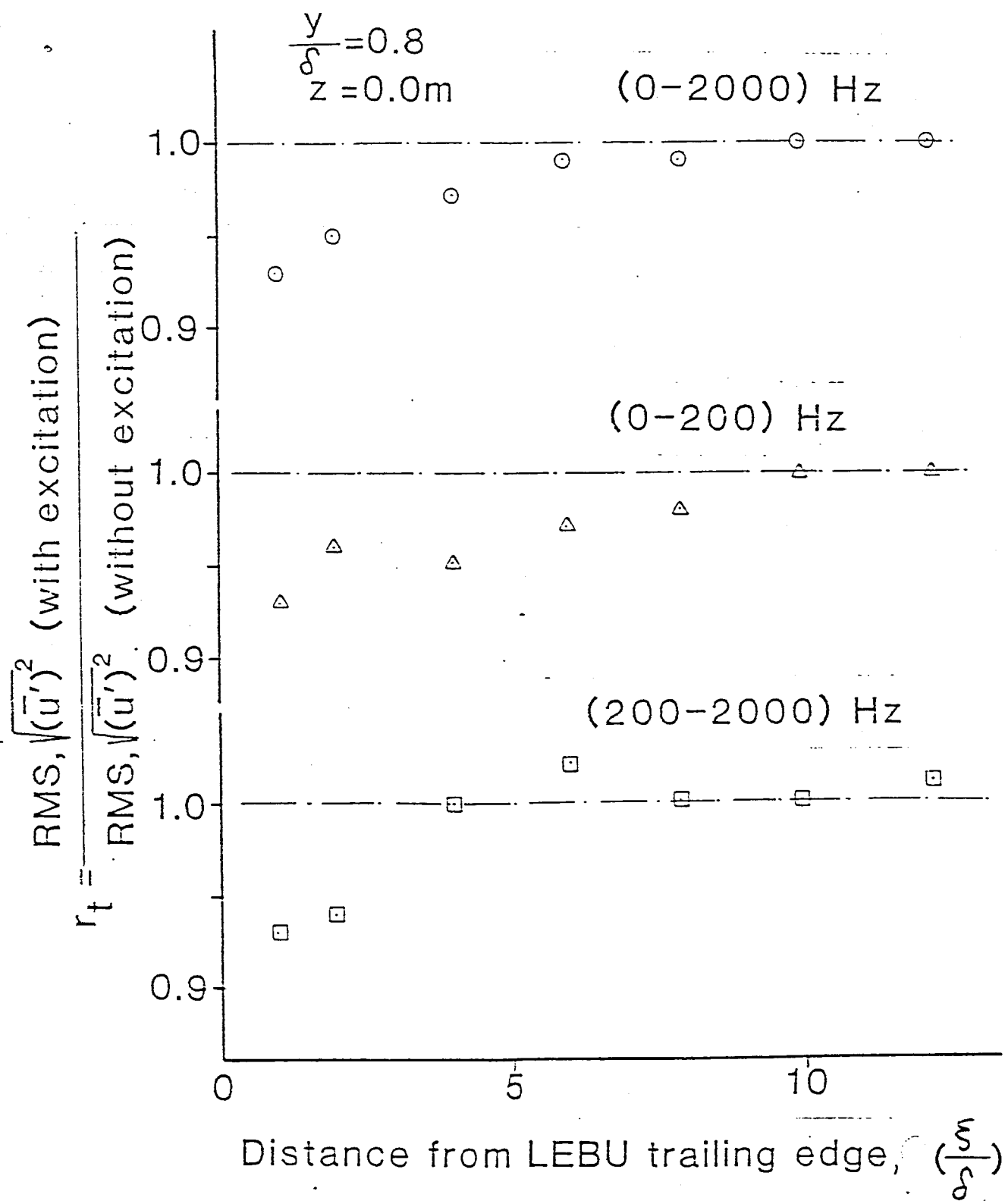


Fig. 10. Relative variation of the low frequency RMS turbulence close to the LEBU trailing edge.

ORIGINAL PAGE IS  
OF POOR QUALITY.

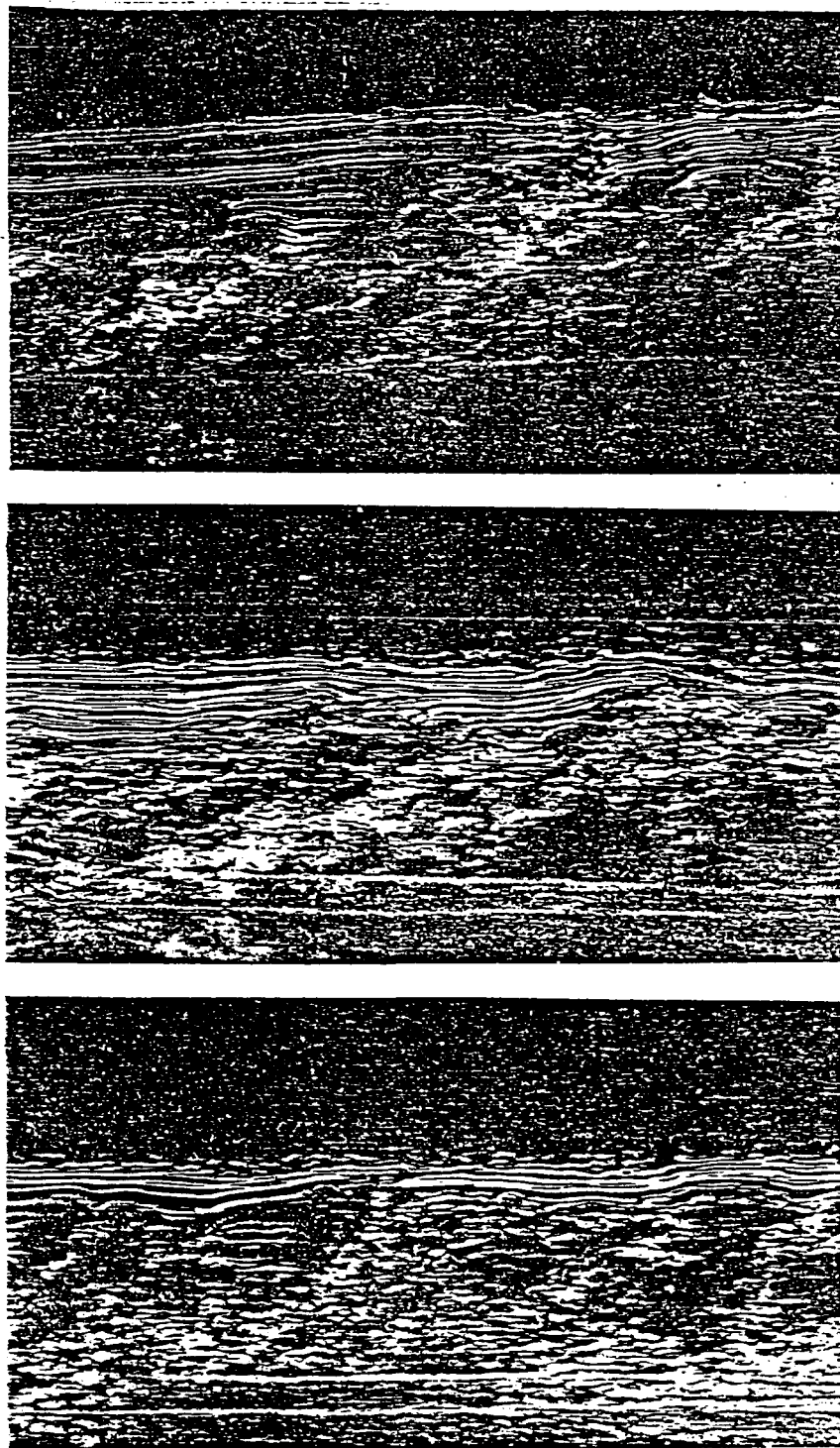


Fig. 11. Boundary layer flow visualization for the: (A) plain case, (B) LEBU manipulated and (C) acoustically excited LEBU configurations.

The results were obtained at approximately 35δ downstream of the manipulator.

The sound waves at the LEBU trailing edge apparently shed vorticity which helps cancel the oncoming large eddies.

The possibility of vertical oscillation of the thin ribbon when 'hit' by acoustic waves was examined. The goal of this study is to control the large eddie break-up process without moving the LEBU. Motion of the device could generate more disturbances in the flow and alter the boundary layer on the device. A small accelerometer was mounted on the LEBU above the acoustic wave input port. Vertical displacement measurements were obtained with no flow; the pressure pulse device was excited with a previously recorded anemometer signal from the turbulent boundary layer. The measured vertical displacement, when acoustics were applied, was indistinguishable from the background electronic noise. The reduced correlation of the flow across the LEBU and reduction of RMS velocity fluctuations with acoustics can be only attributed to the interaction of the acoustic input and the fixed LEBU, not the motion of the manipulator device.

#### Concluding Remarks

According to these results an acoustic pulse of the proper sound pressure level which is phase locked to the convected large scale structure can enhance the effectiveness of a plate manipulator. Large scale eddies contribute approximately 50 percent of the turbulent energy and 80 percent of the Reynolds stress when the outer part of the boundary layer is considered<sup>5</sup>. Turbulent bursting in the sublayer accounts for most of the turbulence and Reynolds stress close to the wall<sup>23,24</sup>. If the passage of the large eddies is related to the triggering of 'bursting' events in the sublayer, then the enhanced large eddy destruction can influence wall events. Energy exchange

between the mean flow and turbulence is also governed by the dynamics of the large eddies<sup>25</sup> which extract kinetic energy from the mean flow. The break-up of the energy cascade process between the very large eddies and the small energy dissipating eddies can therefore lead to reduced skin friction drag.

It should be emphasized that the acoustic input must be phase locked to the convected large eddies and must have a sound pressure level sufficiently high to influence the eddy cancellation. Such an acoustic input: cancels large eddies, reduces the space-time correlation coefficient across the LEBU, reduces the level of low frequency turbulence and reduces the wall skin friction.

#### Acknowledgement

This work has been supported by grant NAG-1-424 from the NASA Langley Research Center. The authors would also like to recognize Mr. Lance Mangum who built the signal processor used to generate the acoustic input.

### References

1. Falco, R. E., "Coherent Motions in the Outer Region of Turbulent Boundary Layer," *The Physics of Fluids*, Vol. 20, No. 10, Pt. 11, October 1977, pp. S 124-S 132.
2. Kovasznay, L. S. G., Kibens, V., and Blackwelder, R. F., "Large-Scale Motion in the Intermittent Region of a Turbulent Boundary Layer," *Journal of Fluid Mechanics* (1970), Vol. 41, pp. 283-325.
3. Corrsin, S. and Kistler, A. L., "Free Stream Boundaries of Turbulent Flows," NACA TR 1244, 1955.
4. Kline, S. J., Reynolds, W. C., Schraub, F. A., and Runstadler, P. N., "The Structure of Turbulent Boundary Layer," *Journal of Fluid Mechanics*, (1967), Vol. 30, Pt. 4, pp. 741-773.
5. Blackwelder, R. F. and Kovasznay, L. S. G., "Time Scales and Correlations in a Turbulent Boundary Layer," *The Physics of Fluids*, Vol. 15, Number 9, Sept. 1972, pp. 1545-1554.
6. Falco, R. E., "The Production of Turbulence Near a Wall," AIAA Paper 1980-1356.
7. Yajnik, K. S. and Acharya, M., "Non-Equilibrium Effects in a Turbulent Boundary Layer Due to the Destruction of Large Eddies," National Aeronautical Laboratory, Bangalore, NAL-BL-7, Aug. 1977.
8. Hefner, J. N., Weinstein, L. M., and Bushnell, D. M., "Large-Eddy Break-up Scheme for Turbulent Viscous Drag Reduction," Symposium on Viscous Drag Reduction, Dallas, Texas, Nov. 7-8, 1979.
9. Corke, T. C., Guezennec, Y., and Nagib, H. M., "Modification in Drag of Turbulent Boundary Layers Resulting from Manipulation of Large Scale Structures," Symposium on Viscous Drag Reduction, Dallas, Texas, Nov. 7-8, 1979.
10. Corke, T. C., Nagib, H. M., and Guezennec, Y., "A New View on Origin, Role, and Manipulation of Large Scales in Turbulent Boundary Layers," NASA CR-165861, Feb. 1982.
11. Bertelrud, A., Truong, T. V., and Avellan, F., "Drag Reduction in Turbulent Boundary Layers using Ribbons," AIAA Paper 82-1370.
12. Plesniak, M. W. and Nagib, H. M., "Net Drag Reduction in Turbulent Boundary Layers Resulting from Optimized Manipulation," AIAA Paper 85-0518.
13. Anders, J. B. and Watson, R. D., "Airfoil Large-Eddy Break-up Devices for Turbulent Drag Reduction," AIAA Paper 85-0520.

14. Hefner, J. N., Anders, J. B., and Bushnell, D. M., "Alteration of Outer Flow Structures for Turbulent Drag Reduction," AIAA Paper 83-0293.
15. Anders, J. B., "Low Reynolds Number LEBU Performance," Drag Reduction and Boundary Layer Control Symposium, National Academy of Science, Washington, D. C., Oct. 1985.
16. Liss, A.Y., and Usoltsev, A.A., "Influence of Vortex-Wing Interaction on Reducing Vortex Induction," Izvestiya Vuz. Aviatsionnaya Technika Vol. 16, No. 3, pp. 5-10, 1973.
17. Guezennec, Y. G. and Nagib, H. M., "Documentation of Mechanisms Leading to Net Drag Reduction in Manipulated Turbulent Boundary Layers," AIAA Paper 85-0519.
18. Nagel, R. T. and Alaverdi, O., "The NCSU Low Speed Boundary Layer Wind Tunnel," SAE Paper 851897, 1985.
19. Papathanasiou, A. G., PhD Dissertation, North Carolina State University, Aerospace Engineering, 1986.
20. White, F. M., Viscous Fluid Flow, McGraw-Hill Book Company, New York, 1974, pp. 503.
21. Melnik, R. E. and Chow, R., "Asymptotic Theory of Two Dimensional Trailing Edge Flows," NASA SP-347, 1979, pp. 177-249.
22. Schlichting, H., Boundary Layer Theory, 7th Edition, McGraw Hill Book Company, New York, 1979, pp. 175-179.
23. Kim, H. T., Kline, S. J., and Reynolds, W. C., "The Production of Turbulence Near a Smooth Wall in a Turbulent Boundary Layer," Journal of Fluid Mechanics (1971), Vol. 50, Pt. 1, pp. 133-166.
24. Lu, S. S. and Willmarth, W. W., "Measurements of the Structure of the Reynold's Stress in a Turbulent Boundary Layer," Journal of Fluid Mechanics (1973), Vol. 60, Pt. 3, pp. 481-511.
25. Tennekes, H. and Lumley, J. L., First Course in Turbulence, Chpt. 3, The MIT Press, Cambridge, 1972.